Research Article | Vol. 29, No. 25 / 6 Dec 2021 / Optics Express 42082
Optics EXPRESS

Supercontinuum lidar for industrial process analysis

ABBA SALEH,[1,2,*] PIOTR RYCZKOWSKI,[1] GOERY GENTY,[1] AND JUHA TOIVONEN[1]

[1] Photonics Laboratory, Physics Unit, Tampere University, P.O. Box 692, FI- 33101 Tampere, Finland
[2] Valmet Technologies Oy, Energy Services, Lentokentankatu 11, P.O. Box 109, FI- 33101 Tampere, Finland
[*] abba.saleh@tuni.fi

Abstract: Real-time monitoring of flue gas parameters in combustion processes is central to the optimization of the process efficiency and reduction of pollutants emission. We report simultaneous measurement of the average water vapor temperature and concentration over a 9 m distance in a full-scale industrial boiler by broadband lidar employing a custom supercontinuum source covering the wavelengths of ro-vibrational absorption of water molecules at 1.2 – 1.55 µm. The measured average temperature and concentration are in excellent agreement with reference measurements. We also take advantage of the backscattering from the aerosol particles present in the boiler to map the water vapor concentration profile in the boiler up to a distance of 2.7 m with a spatial resolution of 30 cm. Our results open novel perspectives for 3D profiling of temperature and gas concentration in industrial environments.

1. Introduction

Global energy demand has tremendously increased over the years, raising environmental concerns. This has led to new energy policies aiming towards renewable energy alternatives and zero net CO_2 fuels such as biomass. The performance of a combustion power plant relies on the internal distribution of its flue gas parameters, such as the temperature and molecular concentrations, and accurate profiling of these parameters would pave the way for optimized combustion process control, increased energy production efficiency and lower emissions.

Conventional approaches for the measurement of flue gas temperature and concentration rely on thermocouple [1] or Fourier transform infrared (FTIR) spectroscopy [2,3]. However, both techniques are inefficient in terms of pointwise measurements. Moreover, the FTIR approach is extractive in nature, yielding significant challenges (latency, moisture content in the gas and ash in the furnace) which makes real-time monitoring of the combustion processes particularly difficult. Flue gas temperature monitoring with a thermocouple is inapplicable to in-situ temperature probing due to the long time constant of the thermocouple response [4] relative to the dynamic temperature distribution of the flue gas. Other optical spectroscopic techniques have been proposed for combustion diagnostics [5–8], however, these typically measure the transmitted signal across a given path between two openings in the furnace walls limiting the measurement area and making them not well-suited to combustion units with limited optical access such as boilers.

Lidar technologies offer novel perspectives for industrial process control and combustion diagnostics. Lidar operation principle is based on time of flight measurement of backscattered electromagnetic radiation [9], enabling remote characterization of flue gas parameters with high spatial resolution [10–12]. Lidar techniques typically use a narrowband laser tuned to the absorption line of the gas of interest, which restricts measurements to a single gas specie. In this context, the development of spatially coherent broadband supercontinuum (SC) light source [13] has opened up new possibilities for simultaneous detection of multiple parameters of flue gas components as shown in a recent demonstration of a laboratory-scale combustion study [14].

#443244 https://doi.org/10.1364/OE.443244
Journal © 2021 Received 13 Sep 2021; revised 16 Nov 2021; accepted 22 Nov 2021; published 2 Dec 2021

Optics EXPRESS

Here, we report real-time combustion diagnostics in a full-scale 9-m-wide industrial boiler via single optical access using a SC-lidar system. Exploiting differential absorption SC spectrum, we demonstrate simultaneous measurement of water vapor temperature and concentration. The average water vapor concentration and temperature are determined using the strong backscattering from the back wall of the boiler. Taking advantage of the backscattering from the aerosol particles naturally present in the boiler, we further map the water vapor concentration along the beam path up to 2.7 m with a resolution of 30 cm limited by the signal-to-noise ratio and SC pulse duration, respectively. Our results demonstrates the unique capability of SC-lidar for diagnosis in combustion units and other industrial environments and open up novel perspective for 3D profiling of temperature and gas concentration in industrial environments.

2. Methodology

We begin by illustrating the temperature and concentration measurement principle of water vapor (H_2O) which is one of the primary flue gas component in a biomass combustion boiler. The transmission spectrum of H_2O in the near-infrared with a typical 20 % concentration, pressure of 1 atm and for an interaction length of 9 m was modeled with high spectral resolution using the HITEMP database [15]. Figure 1 shows the transmission spectrum for two different temperature (400 °C and 900 °C) convoluted to a low spectral resolution for better visualization. One can see how the transmittance depends on the temperature, and this can be advantageously used to determine the gas temperature using three spectral regions as highlighted in the figure: Channel 1 (Ch1), Channel 2 (Ch2), and Channel 3 (Ch3) have corresponding central wavelengths of 1240 nm, 1375 nm and 1500 nm, and full width half maximum (FWHM) of 50 nm, 85 nm and 90 nm respectively. Ch1 is used as a reference channel with negligible water vapor absorption, Ch2 and Ch3 wherein light experiences significant water vapor absorption and which can be used to determine the temperature as described below.

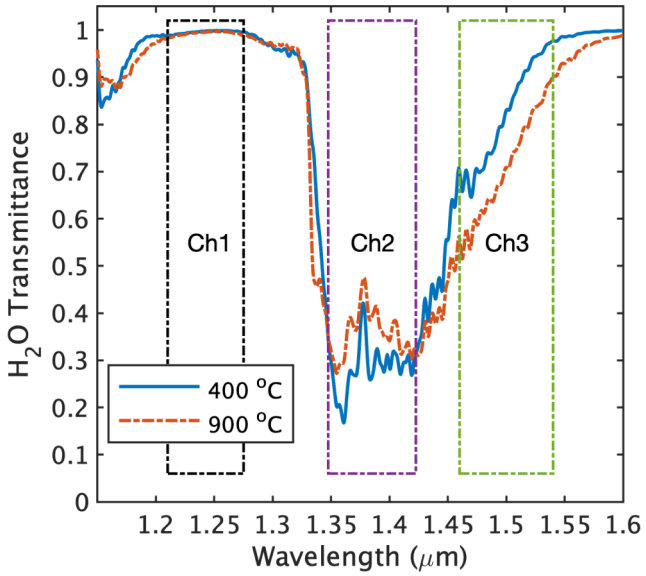

Fig. 1. Modeled H_2O transmittance spectra at two extreme temperatures observed inside a boiler furnace and an overlay of the corresponding wavelength ranges of three specific bandpass filters Ch1, Ch2 and Ch3. Blue (—) and orange (– -) lines are the H_2O transmittance spectra at 400 °C and 900 °C, respectively.

Optics EXPRESS

The backscattered signal $S_n(t_m)$ from Channel $n = 1, 2, 3$ detected after a time of flight t_m can be expressed as [9]

$$S_n(t_m) = \frac{C_{\text{eff}}\beta_m}{{d_m}^2} \int_{\Delta\lambda_n} P_0(\lambda)\Gamma_n(\lambda) \exp\left[-2\sum_{k=1}^{m} \frac{N_k}{V_k}\sigma_k(\lambda, T)\Delta l_k\right] d\lambda, \tag{1}$$

where $\Delta\lambda_n$ is the spectral interval of Channel $n = 1, 2, 3$, d_m is the distance travelled by the backscattered light during time t_m, C_{eff} is the collection efficiency, and β_m is the backscattering coefficient (considered to be wavelength independent as the technique utilizes a relatively small wavelength range of 1.2 – 1.55 µm). The main scattering source is the combustion related fly ash aerosol particles with dimension much larger than the wavelength. $P_0(\lambda)$ is the initial spectrum of the SC source, $\Gamma_n(\lambda)$ is the filter transmission for channel n, and $\sigma(\lambda, T)$ is the absorption cross section dependent on wavelength and gas temperature. $\frac{N_k}{V_k}$ is the molecular number density of the probed gas. The travelled path d_m is divided into elementary segments wherein the temperature and concentration is assumed to be constant. The minimum length of each segment $\Delta l_k = c\tau/2$ is determined by the SC pulse duration τ (c is the speed of light). The first segment parameters are calculated using the initial spectrum of the light source $P_0(\lambda)$. The second segment transmission calculation requires the initial spectrum to be modified by the absorption it experienced in the first segment and the process is then iteratively repeated as the absorption of all preceding segments is known. The total transmittance of individual channels within a given segment can be calculated from

$$T_{n,m} = \frac{S_n(t_{m+1})}{S_n(t_m)}, \tag{2}$$

where $S_n(t_{m+1})$ and $S_n(t_m)$ are the measured backscattered signal at time t_{m+1} and time t_m, respectively. Taking the ratio of transmittance between two different channels does cancel out the effect of d_m^2, C_{eff}, and β_m from the SC-lidar equation assuming that their wavelength dependence is negligible at our operation wavelengths. Knowing the absorption cross section, the light source spctrum as well as the filter transmission spectrum is sufficient to simulate the measured transmittance ratios. The simulated transmittance ratios are formulated to comprise an array of values, calculated using the HITEMP database, and varying temperature and concentration of the gas. The probed gas temperature and concentration are then deduced by fitting the simulated transmittance ratios to the measured ratios using

$$\Delta_{21,m} = \left|\frac{T_{2,m}}{T_{1,m}} - \frac{T_{2,Sim}}{T_{1,Sim}}\right| \tag{3}$$

$$\Delta_{31,m} = \left|\frac{T_{3,m}}{T_{1,m}} - \frac{T_{3,Sim}}{T_{1,Sim}}\right|, \tag{4}$$

where Δ_{21} and Δ_{31} are the resulting difference between the measured and simulated transmittance ratios of Ch2 to Ch1 and Ch3 to Ch1, respectively. Δ_{21} and Δ_{31} are numerically computed based on the simulations and the measured data, and the minimum error point corresponds to the resulted temperature and concentration of the probed gas.

3. Experiment

Measurements were performed at a 9-m-wide fluidized bed biomass boiler with 190 MW thermal power. A schematic illustration of the experiments is shown in Fig. 2. The light source is a SC generating 2-ns-long pulses with 1 kW peak power and repetition rate of 280 kHz (more detailed can be found in Ref. 13). The SC light is collimated with a reflective collimator and directed to the sidewall of the boiler comprising an opening (hatch). Multiple combustion gases including CO_x, NO_x, H_2O and CH_4 are present in the boiler as well as aerosol particles

Optics EXPRESS

distributed throughout the entire volume. The SC light is scattered by the aerosol particles and partially absorbed by the H_2O molecules as it propagates through the boiler. The inside of the furnace walls is covered with soot which strongly scatters the rest of the beam upon incidence on the back end wall. The backscattered light is collected via a receiver telescope lenses (AC508-075-C & AC254-030-C, Thorlabs) and split using a 50:50 beam splitter (BPD254S-G, Thorlabs). Light transmitted by the beam splitter is spectrally filtered into Ch2 (BP-1375-085, Spectrogon) and focused onto a photodetector (ET-3070, EOT). The reflected light by the beam splitter is splitted using another identical beam splitter and spectrally separated into Ch1 and Ch3 with appropriate filters (BP-1240-050 & BP-1500-090, Spectrogon). The bandpass filters are

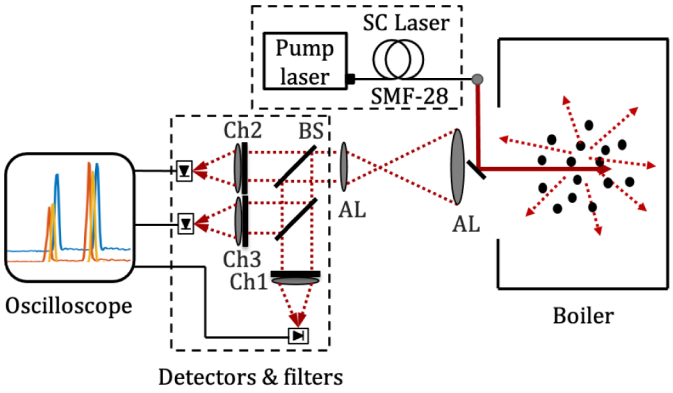

Fig. 2. Layout of experimental arrangement. Abbreviation AL stands for Achromatic Lens, SMF for Single Mode Fiber and BS for Beam Splitter. Ch1, Ch2 and Ch3 are the corresponding bandpass filters for channel 1, 2 and 3, respectively.

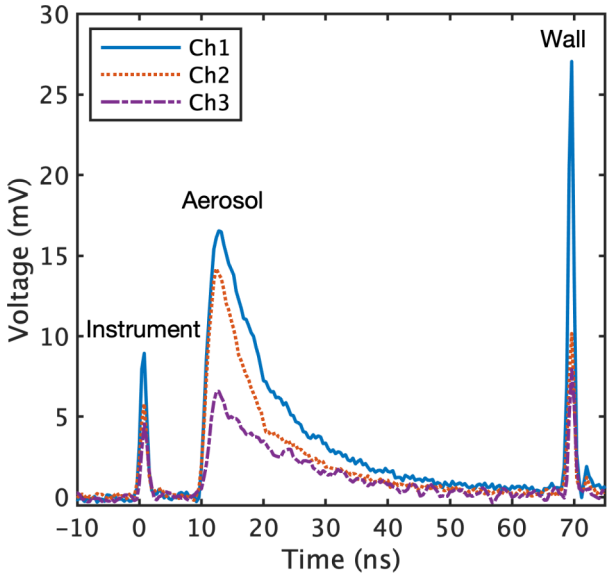

Fig. 3. Measured backscattered SC-lidar signal from a full-scale industrial boiler. The blue (—), orange (· · ·) and purple (- -) lines represent the signals for Ch1, Ch2 and Ch3 respectively. The first and last sharp peaks in the signal corresponds to scattering from the SC source input coupler and the boiler back wall respectively. The signal recorded between 10 ns and 60 ns originates from scattering by the aerosol particles.

Optics EXPRESS

having optical density of 3 at the blocking wavelengths. The corresponding signals are measured with identical photodetectors. The time window of signal collection is triggered by an optical pulse generated by the laser, eliminating the influence of the laser pulse emission time jitter. The signal from each photodetector is preamplified by an electronic amplifier (HSA-Y-1-60, FEMTO) and the temporarily resolved signal is recorded by a 12-bit oscilloscope (HDO6054, Lecroy). Note that SC pulse scattered from different positions inside the furnace arrives at the detector with different time delays, thus encoding spatial dimension onto the temporal signal. An example of recorded signal is shown in Fig. 3. The signal was averaged over sixty-five thousand backscattered pulses recorded over a total measurement time of about 230 ms. Identical measurement time and averaging was used in all our measurements. One can see that the detected signal exhibits three different peaks at different delay times. The first peak in the detected signal near zero-delay represents scattering from the coupling mirror placed in front of the boiler. The broad and slowly decaying peak near 10 ns represents the scattered signal from the aerosol particles. The third peak at around 70 ns delay originates from the boiler back wall reflection.

4. Results and discussion

The average temperature and H_2O concentration in the boiler can be determined from the first (coupling mirror) and last (boiler wall) backscattering peaks of the recorded signal in Fig. 3. The total transmittance across the boiler is derived for the three channels using Eq. (2). Corresponding gas temperature and concentration are then extracted from Eq. (3) and Eq. (4) with solutions for Channel 2 to 1 and 3 to 1 transmission ratios (with respect to simulation) shown in Fig. 4. The global solution is then found at the point of intersection between Δ_{21} and Δ_{31}, yielding 890°C and 20.3% for the average temperature and concentration of the water vapor, respectively. The standard deviation based on 20 consecutive measurement is 50 °C and 0.8 % for the temperature and concentration respectively.

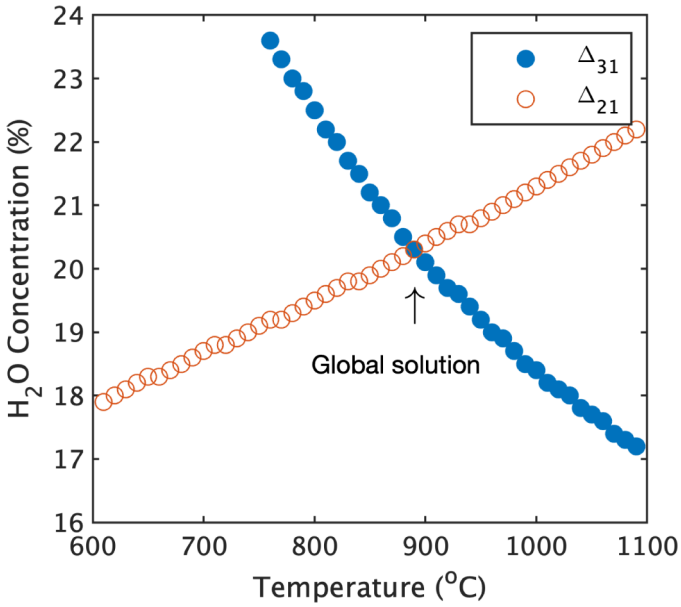

Fig. 4. Minimum error solutions for the difference between the measured (with SC-lidar) and simulated transmittance ratios Δ_{21} and Δ_{31}. Orange (circle) and blue (dot) represents Δ_{21} and Δ_{31} respectively. The global solution can be found at the point of intersection between Δ_{21} and Δ_{31}.

Optics EXPRESS

In order to evaluate the accuracy of our SC-lidar measurements, the results were compared with that of a reference measurement performed using a K-type thermocouple with a maximum penetration depth of about 1.5 m and a 1.045 radiative correction coefficient and the results are shown in Table 1. The estimated average boiler temperature from the thermocouple is 850 °C. The average water vapor concentration was estimated via heat and mass balance calculation [16] utilizing the biomass fuel moisture content measured from oven drying and based on the ISO 18134-3:2015 standard. The resulting average H_2O concentration in the furnace was in the range of 20 – 25 %. These reference measurements agrees very well with the SC-lidar results. It is also important to emphasize that the accuracy of the SC-lidar measurements is perfectly sufficient for industrial-scale process monitoring.

Table 1. Comparison between the reference and SC-lidar measured average temperature and H_2O concentration values in the boiler.

Measurement	Temperature (°C)	H_2O Concentration (%)
Reference	850	20 – 25
SC-lidar	890	20.3

One can take advantage of the backscattered signal from the aerosol particles to spatially resolve the variations in the water vapor temperature and concentration. For this purpose, the measured backscattering signal shown in Fig. 3 is split into discrete segment of 30 cm and the transmittance of each individual segment is derived using Eq. (2). Spatially resolving the gas temperature is infeasible with the current data due to poor signal-to-noise ratio. However, one can solve for the concentration values of the gas by assuming a known temperature, as the relative change in transmission due to temperature variation within a given segment is approximately equivalent to the noise amplitude of the measured signal. Using the reference temperature value of 850 °C across all segments, the H_2O concentration profile in the boiler can be spatially resolved using Eq. (3). The histogram in Fig. 5 shows the retrieved H_2O concentration profile as a function

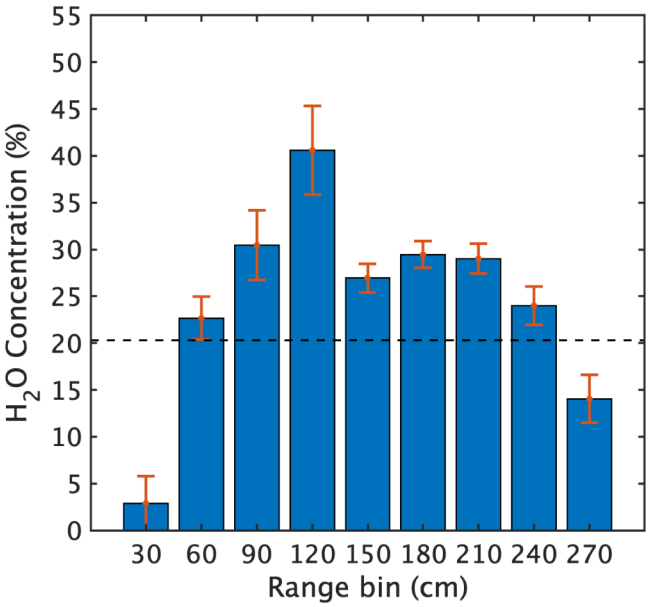

Fig. 5. Spatially resolved H_2O concentration profile and an overlay (– -) of the SC-lidar measured average H_2O concentration in the boiler.

Optics EXPRESS

of distance with the measured average H_2O concentration across the boiler marked as the dashed line. The error bar in the histogram was calculated from twenty consecutive measurements. The measured intensities had about 2 % variation between the measurements. The H_2O concentration values are resolved up to a distance 270 cm into the boiler. Spatially resolving the concentration values at longer distances is limited by the current signal-to-noise ratio of our detection. One can see from Fig. 5 that the H_2O concentration distribution is typically low towards the boiler wall. The hatch (inlet) was kept open during the measurement resulting in mixing with the surrounding air, which in turn alters the initial concentration as well as temperature of the gas at close proximity to the wall.

5. Conclusion and outlook

We have demonstrated robust real-time monitoring of combustion gases using a supercontinuum-lidar. The technique enables simultaneous remote measurement of the gas temperature and concentration via single optical access. Proof-of-concept measurements was demonstrated in a full-scale industrial boiler using three specific wavelength bands in the supercontinuum spectrum. Average temperature and concentration distribution of water vapor across the boiler could be measured with a statistical accuracy of 50 °C and 0.8 %, respectively, which is sufficient for industrial-scale process monitoring. The water vapor concentration profile was further spatially resolved with 30 cm resolution up to a 2.7 m distance inside the boiler, limited by the signal-to-noise ratio. The signal-to-noise ratio also did not allow to spatially resolve the gas temperature as the temperature induced change in transmittance within a given segment is of the same order of magnitude as the noise amplitude. The main origin of noise in this experiment is attributed to the SC source spectrum instabilities, and the readout noise associated with the detectors, amplifiers as well as the oscilloscope. Nevertheless, these challenges can be overcome by optimizing the data acquisition scheme to enhance the signal-to-noise ratio. Specifically, this can be achieved using a fast digitizer with real-time processing capability, enabling continuous averaging of the SC pulses at the repetition rate of the laser as well as by employing a SC source with higher spectral power density. Finally, we emphasize the unique potential of the technique for simultaneous 3D profiling of flue gas temperature and molecular concentrations, which can be realized by steering the incident probe beam using a single opening in a boiler or other similar industrial environment.

Funding. Academy of Finland (320165); Horizon 2020 Framework Programme (722380).

Acknowledgments. A.S acknowledges the support from Finnish Cultural Foundation. The authors would like to express their sincere gratitude to Jaani Silvennoinen and Jari Perälä for organizing the measurement campapaign, and Tampereen Sähkölaitos for making these experiments possible by granting us access to their power plant.

Disclosures. The authors declare no conflicts of interest.

Data availability. Data underlying the results presented in this paper are not publicly available at this time but may be obtained from the authors upon reasonable request.

References

1. D. Bradley and K. Matthews, "Measurement of high gas temperatures with fine wire thermocouples," J. Mech. Eng. Sci. **10**(4), 299–305 (1968).
2. E. Vainio, A. Brink, M. Hupa, H. Vesala, and T. Kajolinna, "Fate of fuel nitrogen in the furnace of an industrial bubbling fluidized bed boiler during combustion of biomass fuel mixtures," Energy & fuels **26**(1), 94–101 (2012).
3. E. Vainio, *Fate of fuel-bound nitrogen and sulfur in biomass-fired industrial boilers* (Åbo Akademi University, PhD thesis, 2014).
4. M. Tagawa and Y. Ohta, "Two-thermocouple probe for fluctuating temperature measurement in combustion–rational estimation of mean and fluctuating time constants," Combust. Flame **109**(4), 549–560 (1997).
5. X. Zhou, J. Jeffries, and R. Hanson, "Development of a fast temperature sensor for combustion gases using a single tunable diode laser," Appl. Phys. B **81**(5), 711–722 (2005).
6. M. Aldén, A. Omrane, M. Richter, and G. Särner, "Thermographic phosphors for thermometry: a survey of combustion applications," Prog. Energy Combust. Sci. **37**(4), 422–461 (2011).

Optics EXPRESS

7. J. Borggren, W. Weng, A. Hosseinnia, P.-E. Bengtsson, M. Aldén, and Z. Li, "Diode laser-based thermometry using two-line atomic fluorescence of indium and gallium," Appl. Phys. B **123**(12), 278 (2017).
8. J. Viljanen, T. Sorvajärvi, and J. Toivonen, "In situ laser measurement of oxygen concentration and flue gas temperature utilizing chemical reaction kinetics," Opt. Lett. **42**(23), 4925–4928 (2017).
9. C. Weitkamp, ed., *Lidar: Range-Resolved Optical Remote Sensing of the Atmosphere*, vol. 102 of *Springer Series in Optical Sciences* (Springer, 2005).
10. B. Kaldvee, J. Bood, and M. Aldén, "Picosecond-lidar thermometry in a measurement volume surrounded by highly scattering media," Meas. Sci. Technol. **22**(12), 125302 (2011).
11. E. Malmqvist, J. Borggren, M. Aldén, and J. Bood, "Lidar thermometry using two-line atomic fluorescence," Appl. Opt. **58**(4), 1128–1133 (2019).
12. E. Malmqvist, M. Brydegaard, M. Aldén, and J. Bood, "Scheimpflug lidar for combustion diagnostics," Opt. Express **26**(12), 14842–14858 (2018).
13. J. M. Dudley, G. Genty, and S. Coen, "Supercontinuum generation in photonic crystal fiber," Rev. Mod. Phys. **78**(4), 1135–1184 (2006).
14. A. Saleh, A. Aalto, P. Ryczkowski, G. Genty, and J. Toivonen, "Short-range supercontinuum-based lidar for temperature profiling," Opt. Lett. **44**(17), 4223–4226 (2019).
15. L. Rothman, I. Gordon, R. Barber, H. Dothe, R. Gamache, A. Goldman, V. Perevalov, S. Tashkun, and J. Tennyson, "Hitemp, the high-temperature molecular spectroscopic database," J. Quant. Spectrosc. Radiat. Transfer **111**(15), 2139–2150 (2010).
16. K. C. Weston, *Energy Conversion* (PSW Publishers, 1992), Chap. 3.